IOP Conf. Series: Materials Science and Engineering **142** (2016) 012090 doi:10.1088/1757-899X/142/1/012090

Modeling the Digging Process of Tree Root System by the Mechanism with Hydropulse Drive

Michael V Drapalyuk[1], Petr I Popikov[1], Roman V Yudin[1], Anatoly A Fomin[2,a], Roman V Chernukhin[3]

[1] Voronezh State University of Forestry and Technologies named after G.F. Morozov, Timiryazeva street 8, Voronezh, Russian Federation, 394087
[2] Institute of engineering and automobile transport, Vladimir State University, Gorky street 87, Vladimir, Russian Federation, 600000
[3] Yurga Institute of Technology, National Research Tomsk Polytechnic University, Leningradskaya street 26, Yurga, Russian Federation, 652055

E-mail: [a] fomin1@mail.ru

Abstract. A mathematical model of the mechanism for digging large-sized seedlings or removing stumps on the undergrowth is developed, which is based on the idea of the root system and surrounding soil, as a combination of plurality of spherical elements, interacting with each other, and the knife mechanism, as a set of elementary surfaces that interact with elements of the stump and soil. The effect of blade vibration on the stump removal efficiency with the help of the model is studied.

1. Introduction

When digging or removing large-sized seedlings or stumps clearance on the undergrowth, roadside and shelter belts, machines of manipulator-type with replaceable technological equipment of discrete action have high efficiency. We proposed a mechanism with hydropulse drive as removable processing equipment for excavators and forestry cranes.

The purpose of this article is to develop a mathematical model of digging large-sized seedlings or stumps clearance in the undergrowth by mechanism with hydropulse drive, which will further assess the effectiveness of the proposed design and parameters of blade vibration in various modes. In the simulation of mechanism, shape and physical characteristics of the stump, forest soil, as well as the interactions of these environments with a knife must be properly represented in the model.

2. Justification and implementation of the process by the mechanism with hydropulse drive.

Timber and forest soil are extremely difficult to simulate by objects because of their typological diversity and large number of physical and mathematical parameters describing it, in particular, the type of soil or wood, humidity, anisotropy, friability, crispness, topography. Model of tree and soil is based on the method of discrete elements; environment is represented as the collection of large number of spherical elements (about 10.000) of small size, which are capable of reacting both between themselves and with the working surfaces of the mechanism.

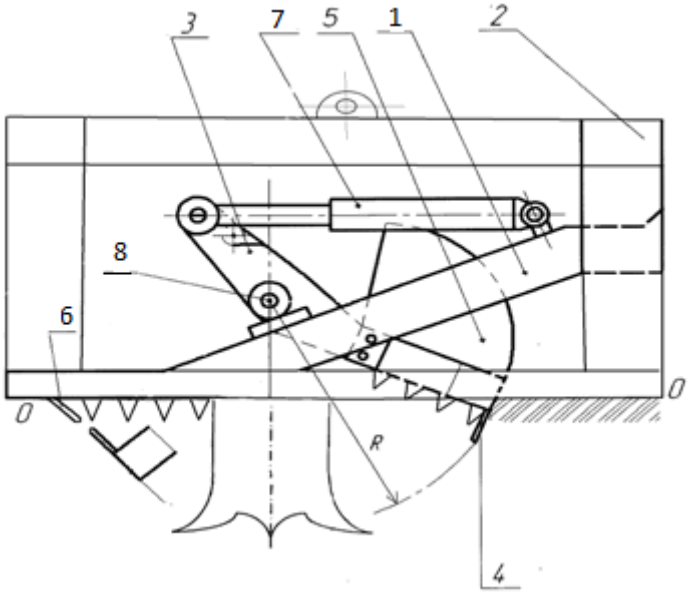

Figure 1. Scheme of mechanism for removing tree stumps: 1 – bearing beams; 2 – frame of mechanism; 3 – vertical rods; 4 – working body; 5 – semi-basket; 6 – spiked bumpers; 7 – hydraulic cylinder; 8 – hinges for mounting vertical rods

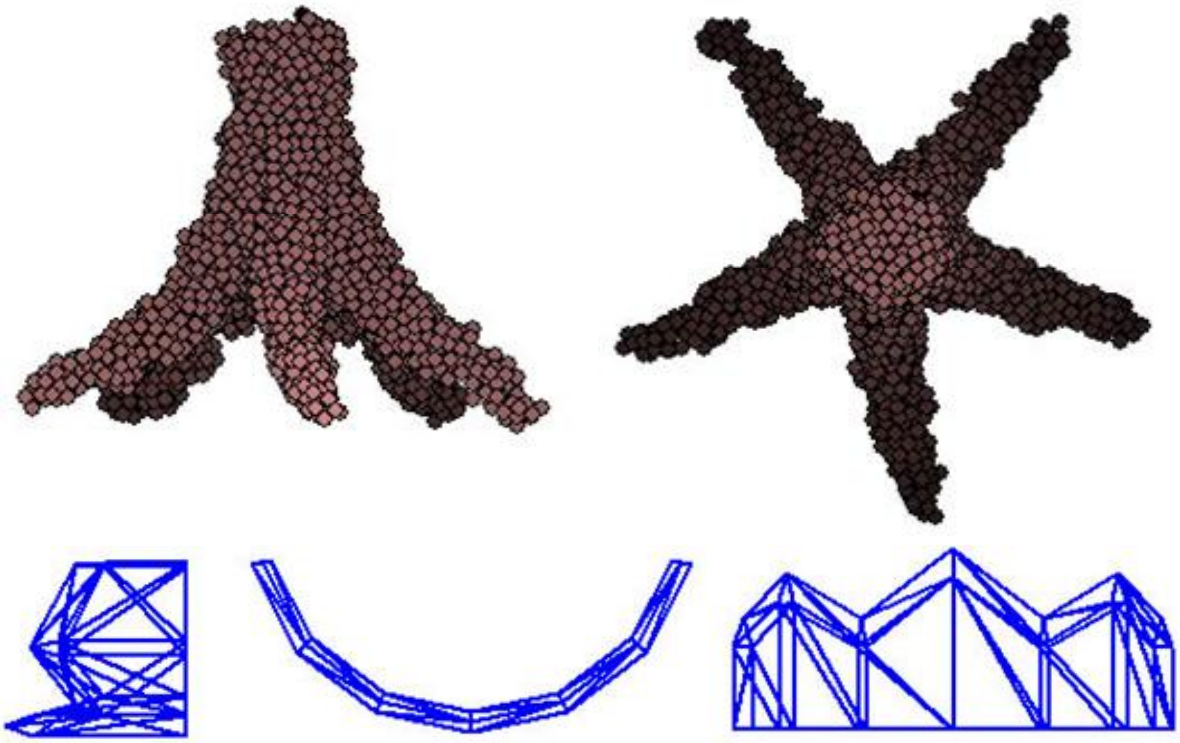

Figure 2. Representation of tree root systems (horizontal and vertical projection) and blade mechanism (three projections) in the model

3. Modeling the digging process of tree root system

The interaction of mechanism working surfaces with wood and soil, from the geometrical point of view, is the problem of finding the distance rв from a plane (the elementary plane of the working surfaces of the mechanism) to the surface of the any spherical element of environment. At this viscoelastic force $\vec{F}_{ij}^{BY}$, acting on the *i*-th element of the soil from the *j*-th element is given by

$$\vec{F}_{ij}^{BY} = c \cdot r_в \cdot \vec{n} - k\vec{v}, \quad (1)$$

where $\vec{n}$ and $\vec{v}$ – direction and speed of the interaction of a ball element and a given surface, calculated for each spherical element of the soil methods of analytic geometry; *c* and *k* - the coefficients of stiffness and viscosity of interaction.

The elastic component of interaction between the elements ensures both the repulsion of elements (distance between centers *rij* of *i*-th and *j*-th elements is less than the element diameter *dE*) and attraction of element over a narrow range of distances ($dE > rij > r\kappa$) (Figure 2), where $r\kappa = \alpha dE$ – critical distance to which elements interact with each other; α – coefficient of expression of critical distance in terms of the diameter the element (in most calculations it took the value of 1.02). When calculating the force $\vec{F}_{ij}$, exerted by the element *i* on the element *j*, it is considered, according to Newton's third law, that the force exerted by the element *j* on the element *i* is the same in magnitude and opposite in direction, i.e. $\vec{F}_{ij} = -\vec{F}_{ji}$. According to Newton's second law, the equations of motion of the *i*-th element are the following:

$$\begin{cases} m_i \dfrac{d^2 x_i}{dt^2} = \sum\limits_{\substack{j=1 \\ j\neq i}}^{N_E} \left(\begin{cases} c_{ij}(d_E - r_{ij})\dfrac{(x_i - x_j)}{r_{ij}} + k_{ij}(r_{ij} - d_{\text{E}})(v_{xi} - v_{xj}), & r_{ij} < d_E + \Delta d_I; \\ 0, & r_{ij} \geq d_E + \Delta d_{\text{I}}; \end{cases} \right) + \sum\limits_{k=1}^{N_s} F^{\text{S}}_{xik}; \\ m_i \dfrac{d^2 y_i}{dt^2} = \sum\limits_{\substack{j=1 \\ j\neq i}}^{N_{\text{E}}} \left(\begin{cases} c_{ij}(d_{\text{Э}} - r_{ij})\dfrac{(y_i - y_j)}{r_{ij}} + k_{ij}(r_{ij} - d_E)(v_{yi} - v_{yj}), & r_{ij} < d_E + \Delta d_I; \\ 0, & r_{ij} \geq d_E + \Delta d_I; \end{cases} \right) + \sum\limits_{k=1}^{N_s} F^{S}_{yik}; \\ m_i \dfrac{d^2 z_i}{dt^2} = -m_i g + \sum\limits_{\substack{j=1 \\ j\neq i}}^{Ne} \left(\begin{cases} c_{ij}(d_E - r_{ij})\dfrac{(z_i - z_j)}{r_{ij}} + k_{ij}(r_{ij} - d_{\text{E}})(v \\ {}_{zi} - v_{zj}), & r_{ij} < d_E + \Delta d_I; \\ 0, & r_{ij} \geq d_E + \Delta d_I; \end{cases} \right) + \sum\limits_{k=1}^{N_S} F^{S}_{zik}, \end{cases} \quad (2)$$

where *i* – element number; m_{i} – mass of the *i*-th element; x_{i}, y_{i}, z_{i} – Cartesian coordinates of the element; *t* – time; N_{E} – quantity of elements; *j* – element number, possibly contacting with the *i*-th element; c_{ij} and d_{ij} – coefficients of stiffness and viscosity of the interaction of elements *i* and *j*; r_{ij} – the distance between the centers of the elements *i* and *j*; v_{xi}, v_{zi} – the Cartesian components of the velocity of *i*-th element; d_{I} – distance of interaction limitations between the elements; *g* – gravitational acceleration; *k* – the number of elementary surface of the mechanism acting on the environment; N_S – the number of elementary surfaces; $F^{\text{S}}_{\text{xik}}$, $F^{\text{S}}_{\text{yik}}$, $F^{\text{S}}_{\text{zik}}$ – Cartesian components of the force exerted by the *k*-th elementary surface on the *i*-th element.

The distance r_{ij} between the centers of the elements is calculated by center coordinates by

Pythagorean Theorem: $r_{ij} = \sqrt{(x_i - x_j)^2 + (y_i - y_j)^2 + (z_i - z_j)^2}$.

When simulating in the model the process of removing the stump pivotal movement of the working body and the vibration transmitted from the hydropulsator to the cylinder takes place. Turning the working body and its vibration are described in the following coordinate transformation of reference points of the elementary surfaces:

$$\begin{cases} x_i' = x_h + r_i \cos(\varphi_i + \omega_w t + \varphi_v \cos(2\pi f_v t)); \\ y_i' = y_i; \\ z_i' = z_h + r_i \sin(\varphi_i + \omega_w t + \varphi_v \cos(2\pi f_v t)); \\ r_i = \sqrt{(x_i - x_h)^2 + (z_i - z_h)^2}; \\ \varphi_i = \begin{cases} \arctan\dfrac{z_i - z_h}{x_i - x_h}, & x_i - x_h \geq 0; \\ \arctan\dfrac{z_i - z_h}{x_i - x_h} + 180^O, & x_i - x\text{h} < 0, \end{cases} \end{cases} \quad (3)$$

where i – index of reference point of elementary surface, which the working body consists of; (x_i, y_i, z_i) and (x_i', y_i', z_i') – coordinates of the i-th reference point before and after the coordinate transformation (in the initial and the current time); (x_h, z_h) – coordinates of axis of the working body passing through the hinges; r_i and φ_i – the polar coordinates of the i-th reference point in the coordinate system associated with the axis of the working body; ω_w – the angular velocity of rotation of the working body; φ_v – vibration amplitude (it is a maximum angle through which the operating element is deflected from the guideline in vibrations); f_v – the frequency of vibration of the working body.

In the proposed version of the model the vibration of the working body is considered only by addition of the term of sum $\varphi_v \cos(2\pi f_v t)$ into the expression for angular position of the working body, however, that already allows to study the influence of the amplitude and frequency of vibration on the stump clearance efficiency.

Blade and limit stop of mechanism are represented in the model as a set of a plurality of elementary triangles (figure 3). Before you start the computer experiment, location of reference points P1 ... P35 is performed in space according to the following formulas, which include the geometric parameters of the blade. After determining the current coordinates of the base points (for this step - time integration τ_i) the construction of the elementary triangles is made that define the working surfaces of the blade and the stop limit. So, for the blade we have the following 54 triangles:

$T_1 = P_1P_2P_{15}$, $T_2 = P_2P_{15}P_{16}$, $T_3 = P_2P_3P_{16}$, $T_4 = P_3P_{16}P_{17}$,
$T_5 = P_3P_4P_{17}$, $T_6 = P_4P_{17}P_{18}$, $T_7 = P_4P_5P_{18}$, $T_8 = P_5P_{18}P_{19}$,
$T_9 = P_5P_6P_{19}$, $T_{10} = P_6P_{19}P_{20}$, $T_{11} = P_6P_7P_{20}$, $T_{12} = P_7P_{20}P_{21}$,
$T_{13} = P_8P_9P_{22}$, $T_{14} = P_9P_{22}P_{23}$, $T_{15} = P_9P_{10}P_{23}$, $T_{16} = P_{10}P_{23}P_{24}$,
$T_{17} = P_{10}P_{11}P_{24}$, $T_{18} = P_{11}P_{24}P_{25}$, $T_{19} = P_{11}P_{12}P_{25}$, $T_{20} = P_{12}P_{25}P_{26}$,
$T_{21} = P_{12}P_{13}P_{26}$, $T_{22} = P_{13}P_{26}P_{27}$, $T_{23} = P_{13}P_{14}P_{27}$, $T_{24} = P_{14}P_{27}P_{28}$,
$T_{25} = P_{15}P_{16}P_{29}$, $T_{26} = P_{16}P_{29}P_{30}$, $T_{27} = P_{16}P_{17}P_{30}$, $T_{28} = P_{17}P_{30}P_{31}$,
$T_{29} = P_{17}P_{18}P_{31}$, $T_{30} = P_{18}P_{31}P_{32}$, $T_{31} = P_{18}P_{19}P_{32}$, $T_{32} = P_{19}P_{32}P_{33}$,
$T_{33} = P_{19}P_{20}P_{33}$, $T_{34} = P_{20}P_{33}P_{34}$, $T_{35} = P_{20}P_{21}P_{34}$, $T_{36} = P_{21}P_{34}P_{35}$,
$T_{37} = P_{22}P_{23}P_{29}$, $T_{38} = P_{23}P_{29}P_{30}$, $T_{39} = P_{23}P_{24}P_{30}$, $T_{40} = P_{24}P_{30}P_{31}$,
$T_{41} = P_{24}P_{25}P_{31}$, $T_{42} = P_{25}P_{31}P_{32}$, $T_{43} = P_{25}P_{26}P_{32}$, $T_{44} = P_{26}P_{32}P_{33}$,
$T_{45} = P_{26}P_{27}P_{33}$, $T_{46} = P_{27}P_{33}P_{34}$, $T_{47} = P_{27}P_{28}P_{34}$, $T_{48} = P_{28}P_{34}P_{35}$,
$T_{49} = P_{15}P_{22}P_{29}$, $T_{50} = P_{21}P_{28}P_{35}$, $T_{51} = P_1P_8P_{15}$, $T_{52} = P_8P_{15}P_{22}$,
$T_{53} = P_7P_{14}P_{21}$, $T_{54} = P_{14}P_{21}P_{28}$ (4)

Stop limit in the model consists of four triangles:

$T_{55} = P_{36}P_{38}P_{39}$, $T_{56} = P_{36}P_{37}P_{39}$, $T_{57} = P_{36}P_{40}P_{41}$, $T_{58} = P_{36}P_{37}P_{41}$.

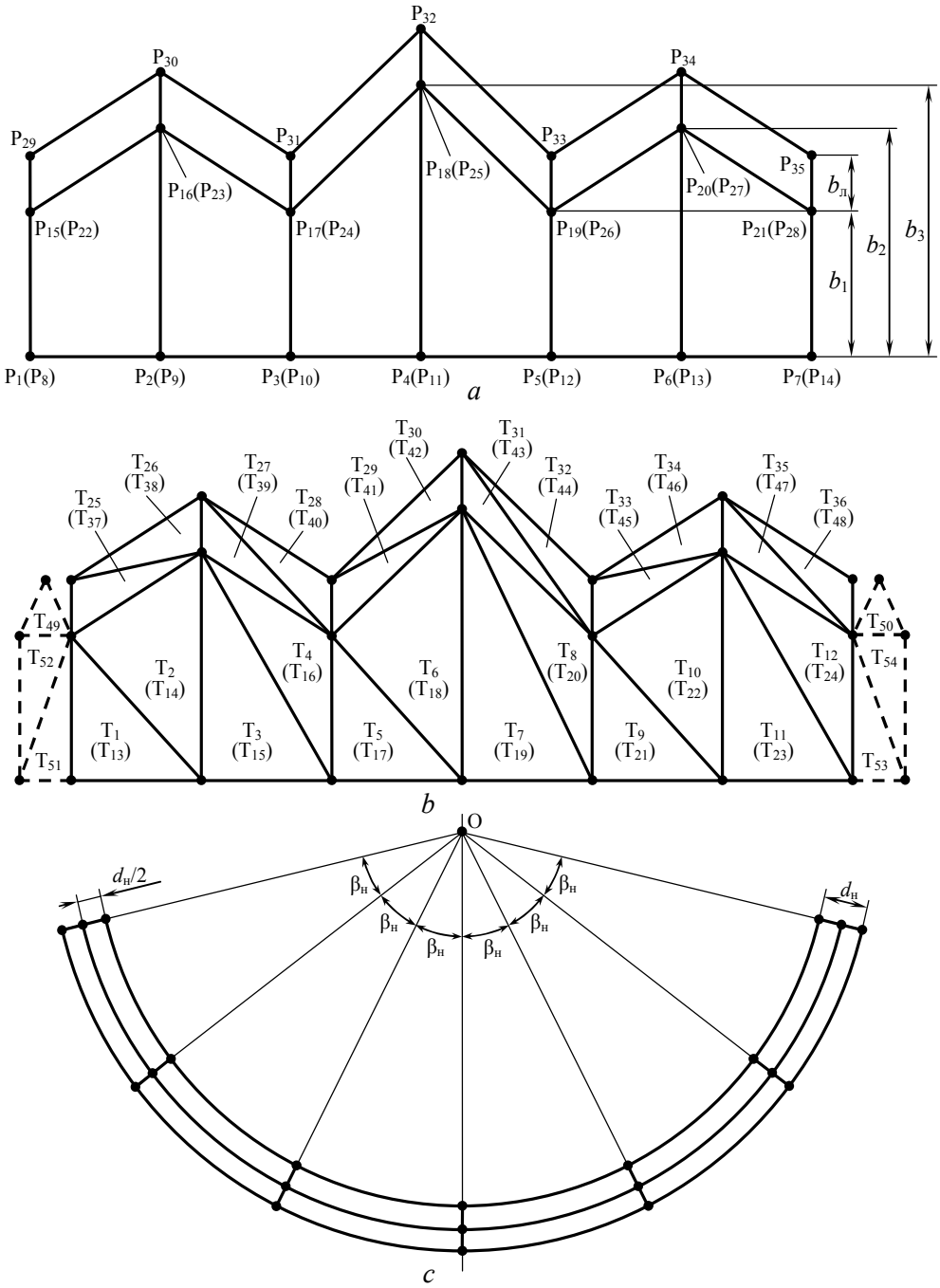

Figure 3. Presentation of blade of mechanism in the model: the basic point Pi (a) and elementary triangles Ti (b) to scan the blade, as well as a view of the front blade (c)

Modeling of hydraulic subsystem is based on analysis of changes in volume V_m of various cavities (m - means the index of the cavity) during the operation of the mechanism. The pressure P_m in the cavity m varies according to the relation:

$$\frac{dP_m}{dV_m} = -\frac{E}{V_m}, \tag{5}$$

where E – bulk modulus of the working fluid.

If pressures in two hydraulically interconnected cavities i and j are different, there is a flow of the

working fluid in the model. The consumption Q_{ij} is determined by the known formula

$$Q_{ij} = k_{ij}\text{sign}(P_i - P_j)\sqrt{|P_i - P_j|}, \quad (6)$$

where i and j – indexes of cavities; k_{ij} – throttling coefficient; sign(x) – function that returns the sign of the variable x.

This formula is used both for throttles (throttling coefficient is sufficiently small), and piping (large throttling coefficient).

In the model it is assumed that all throttling elements have circular cross section, and then the throttling coefficient is determined through orifice diameter d_{ij} by the formula:

$$k_{ij} = \mu\frac{\pi d_{ij}^2}{4}\sqrt{\frac{2g}{\gamma}}, \quad (7)$$

where μ – discharge coefficient; g – gravitational acceleration; γ – relative density of the working fluid.

Ability of pipelines to expand elastically under the influence of pressure in the model is not directly considered, but the elasticity of working fluid is taken into account indirectly, i.e., through the ratio E.

The rotation of the spool and movement of the piston of the hydraulic cylinder causes a change in the volume of considered cavities, so at each step of integration recalculated of volume of cavities takes place.

To solve the system of differential and algebraic equations, which is laid in the basis for the model, a computer program "Program to simulate the operation of the mechanism with hydropulse drive for stumps clearance" is developed. The program is developed in Borland Delphi 7.0 environment, programming language Object Pascal. Before you start the computer experiment the required parameters of blade, geometric and physical and mechanical parameters of the stump, the parameters of the soil, parameters of hydropulsator and hydraulic system can be set. In the process, the program continuously displays a schematic representation of the mechanism of the stump in three dimensions, and performance indicators in numerical and graphical form (figure 4).

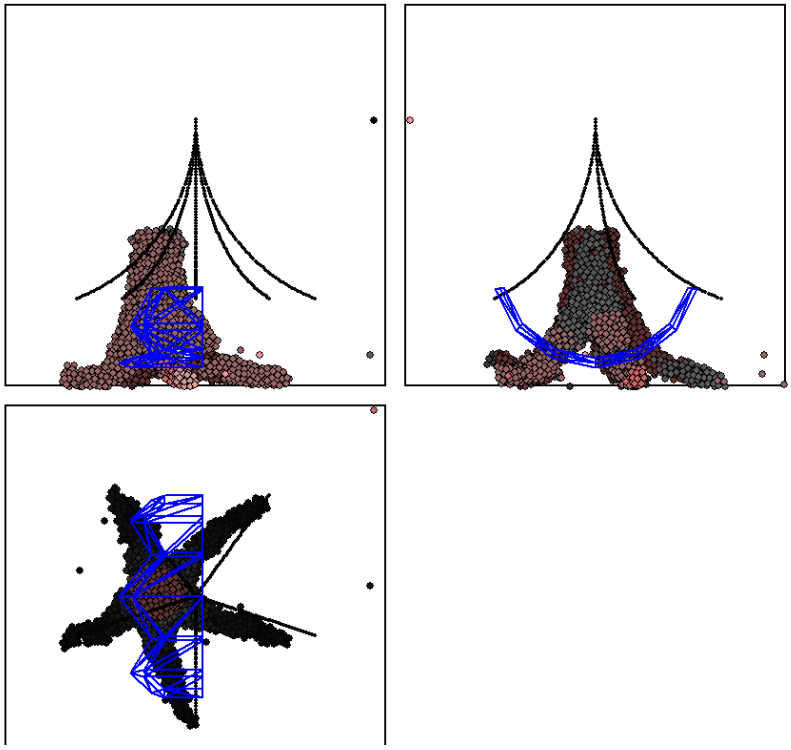

Figure 4. Displaying the simulation results in the developed program

The program is designed for repeated holding of computer experiments on the removal of stumps

with mechanism of a new design and determining the optimal design and technological parameters on this basis.

- The main technical characteristics of the program:
- Number of elements in stump from 2000 to 5000;
- Estimated time of a computer experiment is about 5 minutes (at processor speed 3 GHz).

The first computer experiments have confirmed the effectiveness of the proposed design of the mechanism and efficiency of vibration to improve properties of cutting characteristics of the working body. The model provides a wide range of mechanical properties of the cutting process. In particular, the time dependence of modulus of resistance to the blade deepening was obtained (figure 5) which allows proving optimum shape and thickness of the blade at which the blade has sufficient strength and high cutting properties, but has small thickness and low metal content.

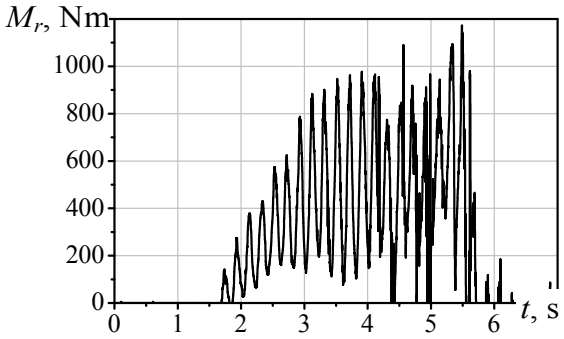

Figure 5. Dependence of the moment of resistance to blade deepening on time

Thus, the mathematical model of the mechanism with hydropulse drive for digging large-sized seedlings or removing stumps on the undergrowth, with its high spatial detail is developed, that allows studying the influence of parameters of blade, vibration, tree root systems and soil on the efficiency of work processes.

References

[1] Fomin, A. A. (2013). Vibrational motion of a complex mill under the action of the cutting force. Russian Engineering Research, 33(1), 57-60.
[2] Thies, W. G., Nelson, E. E., & Zabowski, D. (1994). Removal of stumps from a Phellinus weirii infested site and fertilization affect mortality and growth of planted Douglas-fir. Canadian Journal of Forest Research, 24(2), 234-239.
[3] Compton, J. E., & Boone, R. D. (2000). Long-term impacts of agriculture on soil carbon and nitrogen in New England forests. Ecology, 81(8), 2314-2330.
[4] Palviainen, M., Finér, L., Laiho, R., Shorohova, E., Kapitsa, E., & Vanha-Majamaa, I. (2010). Carbon and nitrogen release from decomposing Scots pine, Norway spruce and silver birch stumps. Forest Ecology and Management, 259(3), 390-398.
[5] Zabowski, D., Chambreau, D., Rotramel, N., & Thies, W. G. (2008). Long-term effects of stump removal to control root rot on forest soil bulk density, soil carbon and nitrogen content. Forest Ecology and Management, 255(3), 720-727.
[6] Morkovina, S. S., Santalova, M. S., Drapalyuk, M. V., & Panyavina, E. A. (2015). Concept of Creation of E-Platforms as Part of Support for Small Innovational Business. Mediterranean Journal of Social Sciences, 6(6), 57.
[7] Page-Dumroese, D. S., Harvey, A. E., Jurgensen, M. F., & Amaranthus, M. P. (1998). Impacts of soil compaction and tree stump removal on soil properties and outplanted seedlings in northern Idaho, USA. Canadian Journal of Soil Science, 78(1), 29-34.

[8] Fomin, A. A., & Gusev, V. G. (2013). Safe machining of blanks with nonuniform properties. Russian Engineering Research, 33(10), 602-606.
[9] Vasaitis, R., Stenlid, J., Thomsen, I. M., Barklund, P., & Dahlberg, A. (2008). Stump removal to control root rot in forest stands: a literature study. Silva Fennica, 42(3), 457-483.
[10] Teketay, D. (1997). The impact of clearing and conversion of dry Afromontane forests into arable land on the composition and density of soil seed banks. Acta Oecologica, 18(5), 557-573.
[11] Rabinowitsch-Jokinen, R., & Vanha-Majamaa, I. (2010). Immediate effects of logging, mounding and removal of logging residues and stumps on coarse woody debris in managed boreal Norway spruce stands. Silva Fennica, 44(1), 51-62.
[12] Prosvirnikov D.B., Ziatdinova D.F., Timerbaev N.F., Saldaev V.A. & Gilfanov K.H. 2016 Mathematical modelling of the steam explosion treatment process for pre-impregnated lignocellulosic material *IOP Conference Series: Materials Science and Engineering* **124**(1), 012087. IOP Publishing. DOI:10.1088/1757-899X/124/1/012087
[13] Iwald, J., Löfgren, S., Stendahl, J., & Karltun, E. (2013). Acidifying effect of removal of tree stumps and logging residues as compared to atmospheric deposition. Forest Ecology and Management, 290, 49-58.
[14] Staaf, H., & Olsson, B. A. (1994). Effects of slash removal and stump harvesting on soil water chemistry in a clearcutting in SW Sweden. Scandinavian Journal of Forest Research, 9(1-4), 305-310.
[15] Hyvönen, R., Olsson, B. A., & Ågren, G. I. (2012). Dynamics of soil C, N and Ca in four Swedish forests after removal of tops, branches and stumps as predicted by the Q model. Scandinavian Journal of Forest Research, 27(8), 774-786.
[16] Fomin, A. A., & Gusev, V. G. (2013). Spindle rigidity in milling blanks with nonuniform properties. Russian Engineering Research, 33(11), 646-648.
[17] Sadrtdinov A.R., Sattarova Z.G., Prosvirnikov D.B. and Tuntsev D.V. (2015, December) Modeling of thermal treatment of wood waste in the gasifiers. In *2015 Int. Conf. on Mechanical Engineering*, *Automation and Control Systems (MEACS)* pp 1-5. DOI:10.1109/MEACS.2015.7414914
[18] Aherne, J., Posch, M., Forsius, M., Lehtonen, A., & Härkönen, K. (2012). Impacts of forest biomass removal on soil nutrient status under climate change: a catchment-based modelling study for Finland. Biogeochemistry, 107(1-3), 471-488.
[19] Prosvirnikov D.B., Safin R.G., Ziatdinova D.F., Timerbaev N.F., and Lashkov V.A. 2016 Multifactorial modelling of high-temperature treatment of timber in the saturated water steam medium. *IOP Conference Series: Materials Science and Engineering* **124**(1), 012088. IOP Publishing. DOI:10.1088/1757-899X/124/1/012088